Focusing Iterative Migration of Magnetic Tensor Field

Zhengwei Xu, University of Houston; Liangjun Yan, Yangtze University; Muran Han, University of Utah; Hemin Yuan, University of Copenhagen; Qianqian Wei, University of Houston.*

SUMMARY

A novel approach for the rapid interpretation of magnetic tensor data is introduced. Magnetic tensor fields are significantly more sensitive to local anomalies than the traditional total magnetic intensity data (TMI). Three-dimensional (3D) iterative magnetic gradient migration is a stable, solid, and alternative technique to solve the disadvantages of inverse problem. The approach can obtain a stable migration image by direct integral transforming an observed tensor field contaminated with a high-noise dataset into a subsurface susceptibility. Moreover, a focusing stabilizing functional is considered into the migration framework to produce more accurate images of distribution of sharp susceptibility anomalies with the correct depth in subsurface formations. An experimental study and a realistic geology model are carried out to investigate the effectiveness of this new method to ascertain how the noise level would influence the stability of migration results. Results show a stable image with high resolution.

INTRODUCTION

Recently, magnetic gradiometers based on superconducting quantum interference devices have been developed and commercially deployed for geophysical surveying (Schmidt et al., 2004; Stolz et al., 2006; Rompel, 2009). It is stressed that since magnetic gradient fields are much more sensitive to the local anomalies than traditional TMI field, so magnetic tensor data is very useful on offering high resolution of imaging susceptibility distribution for interpretation.

In general, 3D inversion, as the only practical technology, is used for quantitative interpretation. However, common interpretation by 3D inversion could be a complex and time-consuming task in calculating and transforming huge matrixes. Moreover, it is very dependent on a priori model as constraint. To overcome the problem, 2D migration of complex magnetic field (Zhdanov et al., 2012) and 3D migration of TMI filed (Wan and Zhdanov, 2013) were introduced to produce smooth 3D rapid imaging of susceptibility distribution without any priori information.

From mathematic point of view, migration field can be presented as the traditional field of the virtual anomalies which is a mirror image of the true one with respect to the real observational surface. Downward continuation of one of the magnetic tensor data components as a special form plays the most important role on magnetic field migration. Hence, compared with traditional downward continuation of the optional field, migration is a stable transform similar as upward continuation.

However, from resolution point of view, firstly, the quality of a migration image would be improved by using iterative migration. Furthermore, traditional migration based on smooth stabilizer functional have disadvantages, especially, in delineating, from a geology point of view, abruptly changing structure boundaries. In this situation, it is useful to find another way to substitute with a stable solution to describe the inverse models with sharp petrophysical boundaries become attractive and critical (Zhdanov, 2002; Zhdanov, 2015). In this paper, we introduce an approach of rapid 3D imaging by magnetic tensor data using focusing iterative migration of magnetic tensor field. This new approach provides a rapid method for direct transformation of the observed magnetic tensor data iteratively into a sharp spatial susceptibility distribution.

In this paper, we present a synthetic study and a realistic geological model for the 3D migration of magnetic tensor data. The purpose of the studies is to see how the noise level would influence the migration results.

ADJOINT OPERATOR AND MIGRAITON FIELD

The basic framework of the expressions of 2D (Zhdanov et al., 2012a) and 3D (Zhdanov et al., 2012b) migration susceptibility is derived from a steepest descent (SD) inversion algorithm. Thus, from mathematic point of view, algorithms of migration and SD have some similarities in formulas derivation, but they are quite different in nature. To better understand how the difference is and the adjoint operator influences the magnetic migration iterative algorithm, we first introduce the SD inversion algorithm. In general, forward problems of magnetic tensor components can be described by the operator equation as follows:

$$\boldsymbol{h}_{\alpha\beta}^{pred} = \boldsymbol{A}_{\alpha\beta}(\boldsymbol{\chi}), \alpha, \beta = x, y, z, \qquad (1)$$

where $\boldsymbol{\chi}$ is an inverted susceptibility model and $\boldsymbol{h}_{\alpha\beta}^{obs}$ a predicted tensor field. $\boldsymbol{A}_{\alpha\beta}$ is a linear operator of a specific magnetic tensor component.

10.1190/segam2019-3214893.1

The *n*-th iteration of the inversion problem solution is given as follows:

$$\boldsymbol{\chi}_{n+1}^{w} = \boldsymbol{\chi}_{n}^{w} + \delta\boldsymbol{\chi}_{n}^{w} = \boldsymbol{\chi}_{n}^{w} - \hat{k}_{n}^{\alpha}\boldsymbol{l}_{n}^{w}, \quad (2)$$

where $\hat{k}_{n}^{\alpha}$ is the step length of each iteration migration based on linear line search and $\boldsymbol{l}_{n}^{w}$ is the weighted direction of the steepest ascent at the nth iteration. $\boldsymbol{\chi}_{n+1}^{w}$ is the weighted susceptibility model. The optimum weighted direction of steepest ascent, $\boldsymbol{l}_{n}^{w}$, satisfies the following normal equation:

$$\boldsymbol{l}_{n}^{w} = \boldsymbol{A}_{\alpha\beta}^{w\,*}\left(\boldsymbol{A}_{\alpha\beta}(\boldsymbol{\chi}_{n}) - \boldsymbol{h}_{\alpha\beta}^{obs}\right) + \alpha\boldsymbol{\chi}_{n}^{w}, \quad (3)$$

where the asterisk (*) denotes a complex conjugate transposed operator (adjoint operator) and $\boldsymbol{A}_{\alpha\beta}^{w}$ the weighted magnetic gradients adjoint operator corresponding to $\boldsymbol{A}_{\alpha\beta}^{*}$.

Applying residual tensor data by the adjoint operator $\boldsymbol{A}_{\alpha\beta}^{*}$, can be defined as the migrated magnetic tensor field as

$$\boldsymbol{H}_{\alpha\beta}^{m} = \boldsymbol{A}_{\alpha\beta}^{*}\left(\boldsymbol{A}_{\alpha\beta}(\boldsymbol{\chi}_{n}) - \boldsymbol{h}_{\alpha\beta}^{obs}\right). \quad (4)$$

So, we can re-write the Equation (2) as:

$$\boldsymbol{\chi}_{n+1} = \boldsymbol{W_m}^{-1}\boldsymbol{\chi}_{n}^{w} - \hat{k}_{n}^{\alpha}\boldsymbol{W_m}^{-2}\boldsymbol{H}_{\alpha\beta}^{m} - \hat{k}_{n}^{\alpha}\alpha\boldsymbol{\chi}_{n}^{w}, \quad (5)$$

where $\boldsymbol{W_m}$ is the depth weighting matrix. Because the migrated field is inversely proportional to the increasing depth, for this reason, it is necessary to apply a suitable spatial weighting function to the migrated magnetic tensor fields to target the correct location of sources of the magnetic tensor fields. To obtain an appropriate weighting operator, the integrated sensitivity of the data to the susceptibility must be used to reconstruct it as follows:

$$\boldsymbol{W_m} = \sqrt{S_{\alpha\beta}} \quad (6)$$

and

$$S_{\alpha\beta} = \frac{\|\delta H_{\alpha\beta}\|_{D}}{\delta\chi}. \quad (7)$$

The expression of integrated sensitivity of each component of the magnetic tensor field is expressed as:

$$S_{zz}(z) = 3H_0\frac{\sqrt{\frac{5\pi}{6}}}{z^3}, \quad (8)$$

$$S_{xx}(z) = S_{yy}(z) = 3H_0\frac{\sqrt{\frac{25\pi}{96}}}{z^3}, \quad (9)$$

$$S_{xy}(z) = S_{yx}(z) = 3H_0\frac{\sqrt{\frac{5\pi}{48}}}{z^3}, \quad (10)$$

$$S_{xz}(z) = S_{zx}(z) = S_{yz}(z) = S_{zy}(z) = 3H_0\frac{\sqrt{\frac{35\pi}{48}}}{z^3}. \quad (11)$$

From the resolution point of view, traditional migration was difficult to use to accurately recover models with sharper geopotential boundaries and contrasts. Thus, in this paper, $\boldsymbol{W_e}$ is introduced as a focusing function using minimum support (MS) (Portniaguine, 2002) to diminish the "smoothness" effect in minimizing the distribution of a discontinuous area with geological properties. After applying the focusing function $\boldsymbol{W_e}$ with the depth weighting function $\boldsymbol{W_m}$, the updated model-depth weighting matrix which was original shown in Eq. 5 can be expressed as

$$\boldsymbol{W_{em}} = \boldsymbol{W_m}\boldsymbol{W_e}, \quad (12)$$

SYNTHETIC STUDY

Figure 1 shows the first 3-D model of two rectangular bodies 200 m wide with a 100 m × 100 m of cross-section area, with susceptibility of 0.04 (SI units) embedded at different depth in a 0 homogeneous half-space. The depth of burial of one of the bodies is 120 m and the one of another is 160 m below the ground surface. The synthetic magnetic tensor field, h_{xx}, h_{xz}, and h_{zz}, in the model is contaminated by 50% random noise and is generated on the surface ($z = 0\ m$).

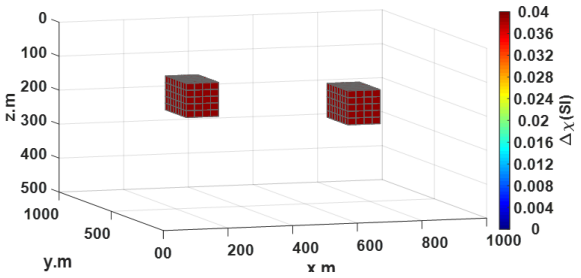

Fig. 1. 3D view of the magnetic model

Figure 2 shows focusing iterative migration results from noise-free (upper panel) and 50% noise (lower panel) using h_{xx} component data. The black dashed lines represent the true location of the anomalous models. One can see that, iterative focusing migration with high noise can produce similar image with the one with noise-free.

10.1190/segam2019-3214893.1

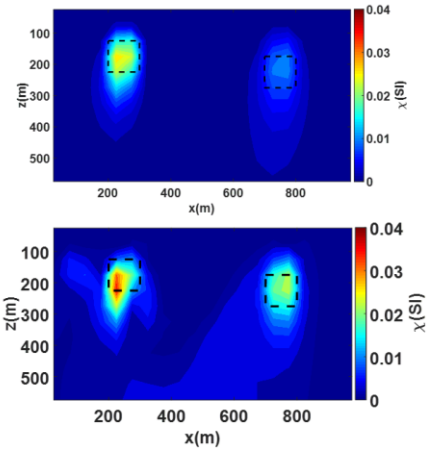

Fig. 2. Iterative migration results using h_{xx} component data along y=500 m. Upper panel: X-Z section view of focusing migration density result with noise-free; Lower Panel: X-Z section view of focusing migration density result with 50% random Gaussian noise.

By using h_{xz} component data, similarity, the focusing iterative migration results from both noise-free (upper panel) and noise (lower panel) is demonstrated in Figure 3. It shows the image with high noise level has similarity with the one without noise. Comparing the Figure. 2, the iterative focusing migration base on h_{xz} component data can produce better image than the h_{xx} component.

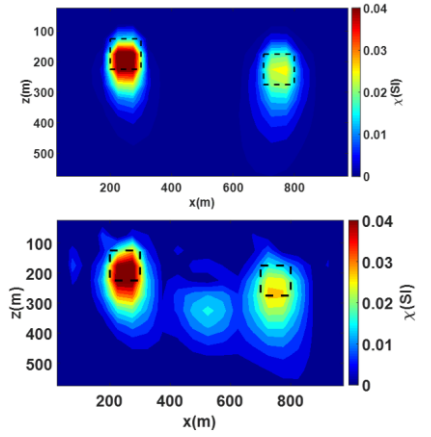

Fig. 3. Iterative migration results using h_{xz} component data along y=500 m. Upper panel: X-Z section view of focusing migration density result with noise-free; Lower Panel: X-Z section view of focusing migration density result with 50% random Gaussian noise.

Figure 4 shows focusing iterative migration results from both noise-free (upper panel) and noise (lower panel) using h_{zz} component data. Comparing with the h_{xx} and h_{xz} components, the model's real position is best reflected by the migration position of result by the h_{zz} component data.

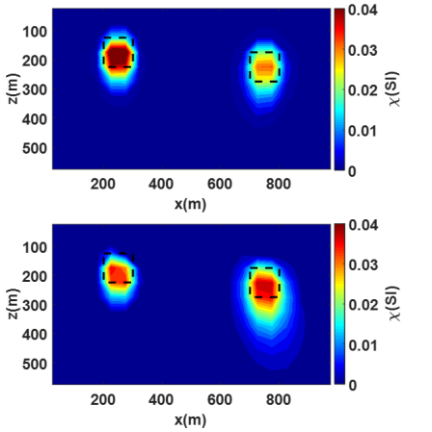

Fig. 4. Iterative migration results using h_{zz} component data along y=500 m. Upper panel: X-Z section view of focusing migration density result with noise-free; Lower Panel: X-Z section view of focusing migration density result with 50% random Gaussian noise.

MASSIVE SULFIDE DEPOSITS MODEL

In this section, we present the results of migration of the magnetic gradient data for the VMS deposits model located at the Bathrust Mining Camp, Canada. In the peripheral area of the cone shown in schematic diagram of the VMS deposit (Figure. 5 upper panel), many minerals with high values of magnetic susceptibility, such as hematite, are associated with noneconomic mineralization. But iron-formation deposits, in which hematite is a common mineral, rarely forms as isolated deposits as it can be temporally and spatially associated with VMS ore body (Peter et al., 2003). As the most commonly component of Zu-bearing mineral, sphalerite of which the magnetic susceptibility is almost zero, is associated with chalcopyrite, pyrite, and pyrrhotite with high magnetic susceptibility show in the conical center deposition area.

In our model study, we have reconstructed a simplified 3D model of VMS based on the schematic diagram shown in Figure. 5 lower panel. In the iterative migration the tolerance was set to 10% random noise level to which our migration converges after just a few iterations. To stand out the effectiveness of the focusing algorithm, we would like to perform smoothing and focusing migration images, respectively. The Fig. 6 shows the migration magnetic susceptibility smooth image (left) and focusing image (right) in the center cross (y=-25 m) for h_{zz}. One can see that the smooth images roughly present the position of the VMS ore body, but the resolution of the images boundaries is blurred and difficult to match the known boundaries. After applying focusing stabilizer, the effect of the focused migration images is better than the smooth one. Furthermore, one can

see that h_{zz} component not only accurately represents the original model, but also the migration value is closer to the true value, especially for the part with high magnetic susceptibility.

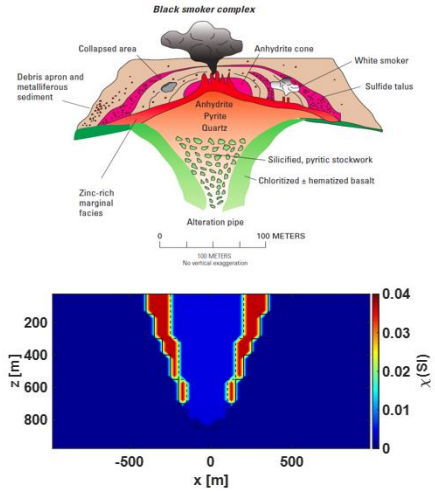

Fig. 5. Upper panel: Schematic diagram of the Volcanogenic Massive Sulfide (VMS) at Bathurst Mining Camp (Hannington et al., 1999); Lower panel: 3D Volcanogenic Massive Sulfide (VMS) model.

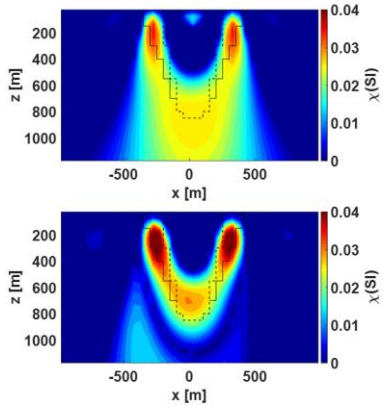

Fig. 6. Migration magnetic susceptibility smooth image (left) and focusing image (right)

CONCLUSIONS

We introduced iterative 3D magnetic tensor field migration to produce 3D magnetic susceptibility distributions by transforming the magnetic gradients directly. The method is based on the theory in which a residual magnetic tensor field can be iteratively transformed to a migration field generated by virtual anomalies that is a mirror image of the true one with respect to the real observational surface. Compared with the traditional downward continuation and first/secondary derivative transformation, magnetic migration is a stable transform since the it is reduced to the downward continuation of analytical function everywhere in the lower half-space without prior information, even under a high level of noise data. In contrast, traditional inversion sometimes could be unstable and nonunique without a prior model as additional constrains.

Furthermore, this also demonstrates that the method produces sharp images after applying with the focusing stabilizer. The reason is, applying the focusing stabilizer, a smooth distribution of all model parameters with a small deviation from the priori model which is set as 0 SI is penalized. However, a focused distribution of the magnetic susceptibility is penalized less. So regardless of whether the observed data is contaminated by noise, the smooth migration does provide less contrast and details as the focusing migration. The experimental study and realistic geological model show that focused migration can not only be stable but can also produce more accurate imaging that reflects correct depth and value information.

ACKNOWLEDEMENT

The study was supported by National Key R&D Program of China (2018YFC0603302) and National Natural Science Foundation of China (U1562109, 41774082).

We are thankful to the Rock Physics Lab (RPL), University of Houston for supporting this research.

10.1190/segam2019-3214893.1

REFERENCES

Hannington, M. D., C. T. Barrie, and W. Bleeker, 1999, The giant kidd creek volcanogenic massive sulfide deposit, western Abitibi Subprovince, Canada — Summary and synthesis, *in* M. D. Hannington, and C. T. Barrie, eds., The Giant Kidd Creek volcanogenic massive sulfide deposit, western Abitibi subprovince, Canada: Economic Geology Monograph 10, 661–672.

Peter, J. M., I. M. Kjarsgaard, and W. D. Goodfellow, 2003, Hydrothermal sedimentary rocks of the heath steele belt, bathurst mining camp, New Brunswick — Part 1. Mineralogy and mineral chemistry, *in* W. D. Goodfellow, S. R. McCutcheon, and J. M. Peter, eds., Massive sulfide deposits of the Bathurst mining camp, New Brunswick, and northern Maine: Economic Geology Monograph 11, 361–390.

Portniaguine, O., and M. S. Zhdanov, 2002, 3-D magnetic inversion with data compression and image focusing: Geophysics, **67**, 1532–1541, doi: https://doi.org/10.1190/1.1512749.

Rompel, A. K. K., 2009, Geologic applications of FTMG: Presented at 11th SAGA Biennial Technical Meeting and Exhibition.

Schmidt, P., D. Clark, K. E. Leslie, M. Bick, D. L. Tilbrook, and C. P. Foley, 2004, GETMAG—a SQUID magnetic tensor gradiometer for mineral and oil exploration: Exploration Geophysics: **35**, 297–305, doi: https://doi.org/10.1071/EG04297.

Stolz, R., V. Zakosarenko, M. Schulz, A. Chwala, L. Fritzsch, H. G. Meyer, and E. O. Kostlin, 2006, Magnetic full-tensor SQUID gradiometer system for geophysical applications: The Leading Edge, **25**, 178–180, doi: https://doi.org/10.1190/1.2172308.

Wan, L.,and M. S. Zhdanov, 2013, Iterative migration of gravity and gravity gradiometry data: 83rd Annual International Meeting, SEG, Expanded Abstracts, 1211–1215, doi: https://doi.org/10.1190/segam2013-1036.1.

Zhdanov, M. S., 2002, Geophysical inverse theory and regularization problems: Elsevier.

Zhdanov, M. S., 2015, Inverse theory and applications in geophysics: Elsevier.

Zhdanov, M. S., X. Liu, G. A. Wilson, and L. Wan, 2012. 3D migration for rapid imaging of total-magnetic-intensity data: Geophysics, **77**, no. 2, J1–J5, doi: https://doi.org/10.1190/geo2011-0425.1.